

See discussions, stats, and author profiles for this publication at: <https://www.researchgate.net/publication/44627880>

# Propene Oxidation on V<sub>4</sub>O<sub>11</sub>- Cluster: Reaction Dynamics to Acrolein

ARTICLE *in* THE JOURNAL OF PHYSICAL CHEMISTRY A · JUNE 2010

Impact Factor: 2.69 · DOI: 10.1021/jp1002947 · Source: PubMed

---

CITATIONS

7

READS

47

## 3 AUTHORS:



Hai-Bei Li

Shandong University

32 PUBLICATIONS 235 CITATIONS

[SEE PROFILE](#)



Shan Xi Tian

University of Science and Technology of C...

88 PUBLICATIONS 713 CITATIONS

[SEE PROFILE](#)



Jinlong Yang

University of Science and Technology of C...

510 PUBLICATIONS 11,060 CITATIONS

[SEE PROFILE](#)

# Propene Oxidation on $\text{V}_4\text{O}_{11}^-$ Cluster: Reaction Dynamics to Acrolein

Hai-Bei Li, Shan Xi Tian,\* and Jinlong Yang

Hefei National Laboratory for Physical Sciences at the Microscale, Department of Chemical Physics, University of Science and Technology of China, Hefei, Anhui 230026, China

Received: January 12, 2010; Revised Manuscript Received: May 12, 2010

Oxidation dynamics of propene ( $\text{CH}_3\text{CH}=\text{CH}_2$ ) to acrolein ( $\text{CH}_2=\text{CHCHO}$ ) on the anionic vanadium oxide cluster  $\text{V}_4\text{O}_{11}^-$  is investigated with the first-principle density functional calculations, providing an interpretation to  $\text{V}_4\text{O}_{11}^- + \text{propene} \rightarrow \text{V}_4\text{O}_{10}\text{H}_2^- + \text{C}_3\text{H}_6\text{O}$  observed in the photochemical reactions (Li, S.; Mirabal, A.; Demuth, J.; Wöste, L.; Siebert, T. *J. Am. Chem. Soc.* **2008**, *130*, 16832). The complicated energy surface of the reaction between  $\text{V}_4\text{O}_{11}^-$  and propene is explored, and the stepwise dynamic processes for propene to acrolein are proposed. Initially, propene is captured by  $\text{V}_4\text{O}_{11}^-$  with a hydrogen bond CH (methyl group in propene)…O (dioxo group in  $\text{V}_4\text{O}_{11}^-$ ), then undergoes dehydrogenation along this hydrogen bond to form a  $\pi$ -allyl radical. After the redehydrogenation of the  $\pi$ -allyl and oxygen transfer from the vanadium oxide cluster, acrolein is eventually produced together with four isomers of  $\text{V}_4\text{O}_{10}\text{H}_2^-$  in the different reaction paths. During this process, the negative charge is found to transfer between the hydrocarbon and the vanadium oxide moieties.

## 1. Introduction

Vanadium oxides are of great interest to many researchers because of their potential industrial and catalytic applications.<sup>1–5</sup> The cluster models of surface catalysis are usually studied toward understanding of its catalytic dynamics, in particular, a lot of studies both of experiments and of theoretical calculations have been carried out to reveal the relationships between chemical reactivity and structure of the cationic,<sup>6</sup> neutral,<sup>6c,g,7</sup> and anionic<sup>6c,8</sup> vanadium oxide clusters. Recently, Li and co-workers found the unique chemical reactivity between  $\text{V}_4\text{O}_{11}^-$  cluster and propene in the photochemistry experiments where the predominant products were  $\text{V}_4\text{O}_{10}^-$  and  $\text{C}_3\text{H}_6\text{O}$ .<sup>8</sup> Propylene oxide, as the more possible product of  $\text{C}_3\text{H}_6\text{O}$ , was further proposed in our recent work with the first principle calculations.<sup>9</sup> Another minor reaction channel to  $[\text{V}_4\text{O}_{10}\cdot\text{H}_2]^-$  and  $\text{C}_3\text{H}_4\text{O}$  was found in the mass spectrometry study, but without any characterizations to the products.<sup>8</sup> In the present computational study, the oxidation product  $\text{C}_3\text{H}_4\text{O}$  is proposed to be acrolein accompanying four possible isomers of  $[\text{V}_4\text{O}_{10}\cdot\text{H}_2]^-$  (as shown in Scheme 1).

The oxidation of propene to acrolein received much attention owing to its role in oxidation catalysis process of the petrochemical industry.<sup>10,11</sup> A great deal of efforts have been made on the searching for efficient catalysts since the 1960s.<sup>12–19</sup> Some multiple metal oxides, such as Fe–Sb–Ti–O,<sup>14</sup> Co–Fe–Mo–O,<sup>16</sup> and Bi–Mo–O,<sup>18</sup> were found, but very few were known about the catalytic oxidation mechanism of propene to acrolein.<sup>11a,20</sup> Experimentally, Aso and co-workers suggested that the acrolein formation proceeded via the interaction of a propene molecule with two surface oxygen atoms.<sup>21</sup> One surface oxygen abstracts a methyl hydrogen from propene while the other surface oxygen is subsequently attracted.<sup>21</sup> The latter was proposed to be the rate-determining step.<sup>21</sup> However, Keulks et al.<sup>22</sup> suggested that the rate-determining step was the abstraction of a methyl hydrogen from propene to form a  $\pi$ -allyl species,

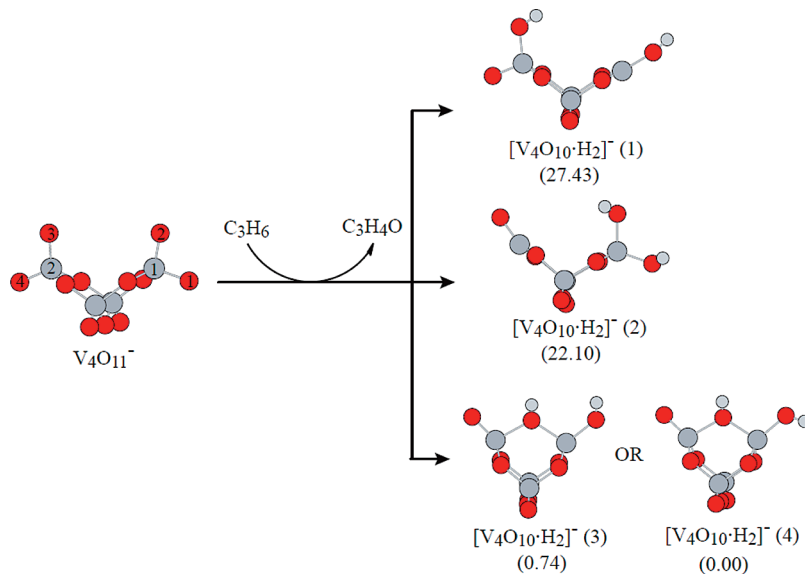
then the oxygen addition led to a  $\sigma$ -allyl intermediate before the second hydrogen abstraction from the  $\pi$ -allyl species. A so-called Mars–van Krevelen reaction mechanism was proposed for the propene oxidation to acrolein: the methyl hydrogen of propene is initially abstracted to form a symmetric allyl radical intermediate that subsequently reacts with lattice oxygen of the catalyst.<sup>18,23–26</sup> On the other hand, some researchers suggested that the catalyst surface (Fe/Sb oxides) in a partially reduced state should be beneficial to produce acrolein;<sup>27</sup> On the contrary, van Steen et al.<sup>28</sup> suggested that the catalyst at a high oxidation state should be beneficial for the high activity and selectivity. To date, there is still lack of agreement on the reaction mechanism and continues to be uncertainties concerning the structure of the reactive intermediates, the nature of the active sites, and the catalyst selectivity.

To elucidate the reaction dynamic mechanisms of propene oxidation to acrolein in heterogeneous catalyzed reaction, the theoretical methods are being applied to have more insights into the mechanistic details of the reactions.<sup>29,30</sup> There are very few reports<sup>31</sup> prior to this work on the oxidation of propene to acrolein catalyzed with the vanadium oxides. The aggregate complex  $[\text{V}_4\text{O}_{11}\cdot\text{C}_3\text{H}_6]^-$  obtained in the photoinduced experiment<sup>8</sup> can be an excellent cluster model in exploring this reaction dynamics. Although the structure of  $\text{V}_4\text{O}_{11}^-$  cluster is different from the surface of vanadium oxides,  $\text{V}_4\text{O}_{11}^-$  can be considered as the cluster model of the oxygen-rich and negatively charged surface of the vanadium oxides.

## 2. Computational Details

The first-principle density functional calculations were carried out with Gaussian 03 suite of program.<sup>32</sup> The Becke three-parameter hybrid functional combined with Lee–Yang–Parr (LYP) correlation functional (B3LYP)<sup>33</sup> was employed together with the triple- $\zeta$  plus polarization basis sets TZVP<sup>34</sup> in the calculations. The B3LYP/TZVP method has been proved to be reliable for vanadium oxides in comparison between the available experimental data and the theoretical results.<sup>6a–e,g,h,7</sup> Four low-lying isomers of  $\text{V}_4\text{O}_{11}^-$  have been reported in the

\* To whom correspondence should be addressed. E-mail: sxian@ustc.edu.cn.

**SCHEME 1:** Four Stable Structures of [V<sub>4</sub>O<sub>10</sub>•H<sub>2</sub>]<sup>-</sup> after the Reaction of Propene on V<sub>4</sub>O<sub>11</sub><sup>-</sup> Cluster

previous literature,<sup>35</sup> and one of two most stable structures was fully reoptimized in this work.<sup>36</sup> More computations were performed for the high-spin (quartet) state of anionic V<sub>4</sub>O<sub>11</sub><sup>-</sup> clusters, indicating they are about 35 kcal/mol higher in energy than the low-spin (doublet) state. Here we will focus on the reactions on the low-spin potential energy surface. The analytic Hessians were calculated to identify each local minimum and transition state (TS). The local minima had no imaginary frequencies, whereas each TS structure was confirmed to be a first-order saddle point with only one imaginary frequency. The harmonic vibrational frequencies were also used in the calculations of zero-point energy (ZPE). Furthermore, the intrinsic reaction coordinate (IRC) method<sup>37</sup> was applied in examinations that each TS structure connected two appropriate local minima in the respective reaction pathway. The reaction enthalpy ( $\Delta H$ ) and Gibbs free energy ( $\Delta G$ ) were calculated at temperature  $T = 298$  K.

To find the roles of the negative charge in the reactions, the charge-density difference maps of the reactants, TS structures, the intermediates, and the products were plotted. These charge-density differences were calculated as,

$$\Delta\rho = \rho_{\text{anion}}^{\text{A}} - \rho_{\text{anion}}^{\text{N}}$$

where  $\rho^{\text{A}}$  and  $\rho^{\text{N}}$  represented the electron density distributions of the anionic and neutral species, respectively. The footnote “anion” denoted the anionic structures that were used through the above calculations.

### 3. Results and Discussion

**Results.** In our previous work, the reactions between V<sub>4</sub>O<sub>11</sub><sup>-</sup> with propene have been clarified using the same method and basis set.<sup>9</sup> The main product C<sub>3</sub>H<sub>6</sub>O<sup>8</sup> was identified as propylene oxide.<sup>9</sup> In that reaction, due to the strong electron withdrawing effect of the methyl group, the covalent bond is formed between the terminal negatively charged oxygen atom in V<sub>4</sub>O<sub>11</sub><sup>-</sup> and the carbon atom (any one in C=C bond) in propene.<sup>9</sup> A weak peak assigned with the product [V<sub>4</sub>O<sub>10</sub>•H<sub>2</sub>]<sup>-</sup> was observed in the mass spectrometry study.<sup>8</sup> We anticipated that the reactions to [V<sub>4</sub>O<sub>10</sub>•H<sub>2</sub>]<sup>-</sup> could be more complicated than those to C<sub>3</sub>H<sub>6</sub>O

+ [V<sub>4</sub>O<sub>10</sub>]<sup>-</sup>.<sup>9</sup> As shown in Scheme 1, [V<sub>4</sub>O<sub>10</sub>•H<sub>2</sub>]<sup>-</sup> has four stable isomers as the products of the reactions proposed in this work. [V<sub>4</sub>O<sub>10</sub>•H<sub>2</sub>]<sup>-</sup> (**1**) and [V<sub>4</sub>O<sub>10</sub>•H<sub>2</sub>]<sup>-</sup> (**2**) show the open structures with two terminal OH groups; and [V<sub>4</sub>O<sub>10</sub>•H<sub>2</sub>]<sup>-</sup> (**3**) and [V<sub>4</sub>O<sub>10</sub>•H<sub>2</sub>]<sup>-</sup> (**4**) are two tautomers with the different orientations of one OH group and show the caged-like structures and. As depicted in Figures 1, 3, 5, we have identified four parallel reaction pathways (paths 1–4, respectively) for the oxidation of propene to acrolein on the anionic V<sub>4</sub>O<sub>11</sub><sup>-</sup> cluster. Path 4 (shown in Figure 5 with the broken thick lines) is very similar to path 3. In order to inspect the charge-transfers between the vanadium oxide cluster and the hydrocarbon, the charge-density difference maps for paths 1, 2, and 3 are shown in Figures 2, 4, and 6, respectively. The optimized geometries of all structures are given as the Supporting Information.

**Methyl Hydrogen Activation.** The geometrical parameters of anionic cluster V<sub>4</sub>O<sub>11</sub><sup>-</sup> are extremely similar with the previous results (see refs 9 and 35). The terminal vanadyl V<sub>1</sub>—O<sub>1</sub> (the atomic labels are given in Scheme 1) group plays a more important role than other terminal ones in the activation of the methyl C—H bond of propene. The charge-density difference maps (see Figures 2, 4, and 6) show that the negative charge is localized at the two terminal O<sub>1</sub> and O<sub>2</sub> atoms, in particular, the most at O<sub>1</sub> atom (also discussed in ref 9). Thus, the O<sub>1</sub> atom has a radical-anion nature,<sup>38</sup> namely, it is active site to be attacked by the positively charged methyl group in propene. In four reaction paths, the hydrogen bond formation C—H···O<sub>1</sub>=V<sub>1</sub> is anticipated to be the start step. Thus the V—O bond length is an important parameter. In the isolated V<sub>4</sub>O<sub>11</sub><sup>-</sup> cluster, the bond lengths of V<sub>1</sub>—O<sub>1</sub> and V<sub>1</sub>—O<sub>2</sub> are 1.722 and 1.631 Å, respectively; the bond lengths both of V<sub>2</sub>—O<sub>3</sub> and V<sub>2</sub>—O<sub>4</sub> are 1.607 Å. At the start steps, the terminal V<sub>1</sub>—O<sub>1</sub> bond as the catalytic active site should be elongated due to the attraction by C—H in the methyl group. However, we cannot find a stable configuration of the weak hydrogen-bonding complex [V<sub>4</sub>O<sub>11</sub>•C<sub>3</sub>H<sub>6</sub>]<sup>-</sup>, implying that this complex might be on an extremely flat potential energy surface and that the C—H···O<sub>1</sub>=V<sub>1</sub> hydrogen bond is too weak. This may be the main reason that the oxidative dehydrogenation of propene to produce [V<sub>4</sub>O<sub>10</sub>•H<sub>2</sub>]<sup>-</sup> is observed as the minor process in the experiments.<sup>8</sup>

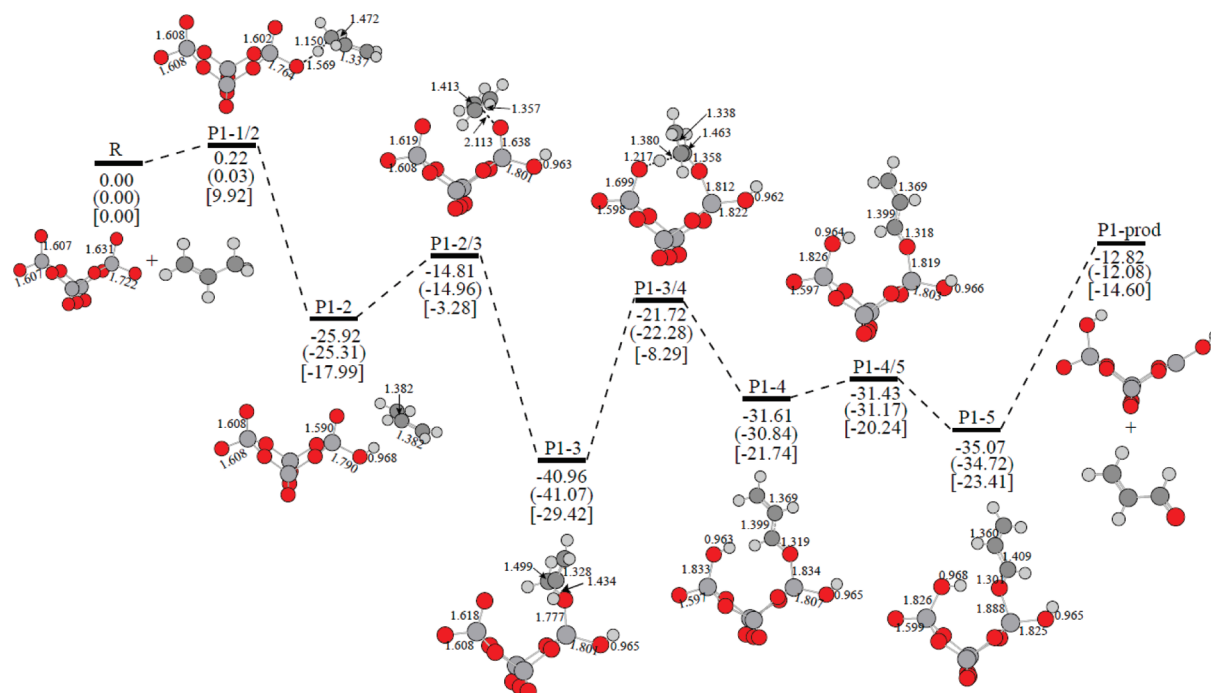


**Figure 1.** The stepwise reactions for path 1. The top energy is the  $\Delta E$  (including ZPE corrections), the middle is  $\Delta H$ , and the bottom is  $\Delta G$ . All reported values are in kcal/mol. Bond distances are shown in angstrom.

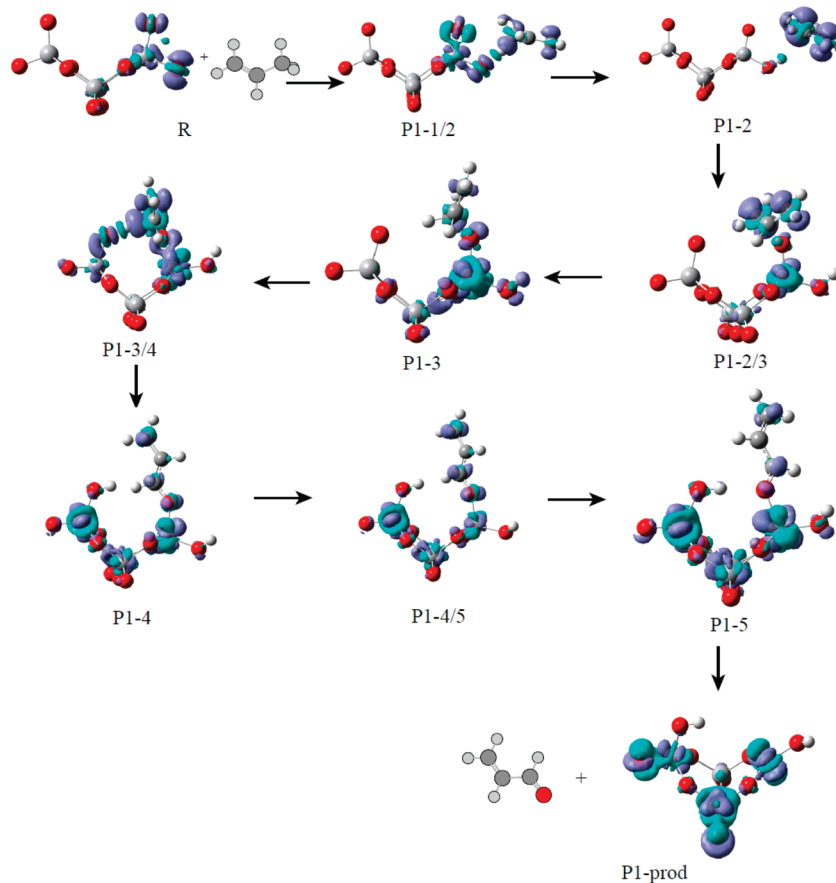


**Figure 2.** Maps of the charge-density difference in the progression of path 1.

For all the paths, the first step in the oxidation of propene is the abstraction of a hydrogen atom from the methyl group in propene. In path 1 (see Figure 1), the TS structure, P1-1/2, shows that a methyl hydrogen coordinates O1 atom and the  $O_1 \cdots H$  distance is 1.569 Å. This transition state has one imaginary frequency of  $\nu = 179i$  cm<sup>-1</sup>, with the vibrational

mode corresponding to the hydrogen abstraction motion by the terminal O1 atom. In this structure, the  $V_1=O_1$  and C–H bonds have been elongated to 1.764 and 1.150 Å, respectively. With respect to the isolated reactants, propene and  $V_4O_{11}^-$ , the activation energy  $\Delta E^\ddagger$  for this first hydrogen abstraction is 0.22 kcal/mol,  $\Delta G^\ddagger$  is 9.92 kcal/mol, and  $\Delta H^\ddagger$  is only 0.03 kcal/mol.

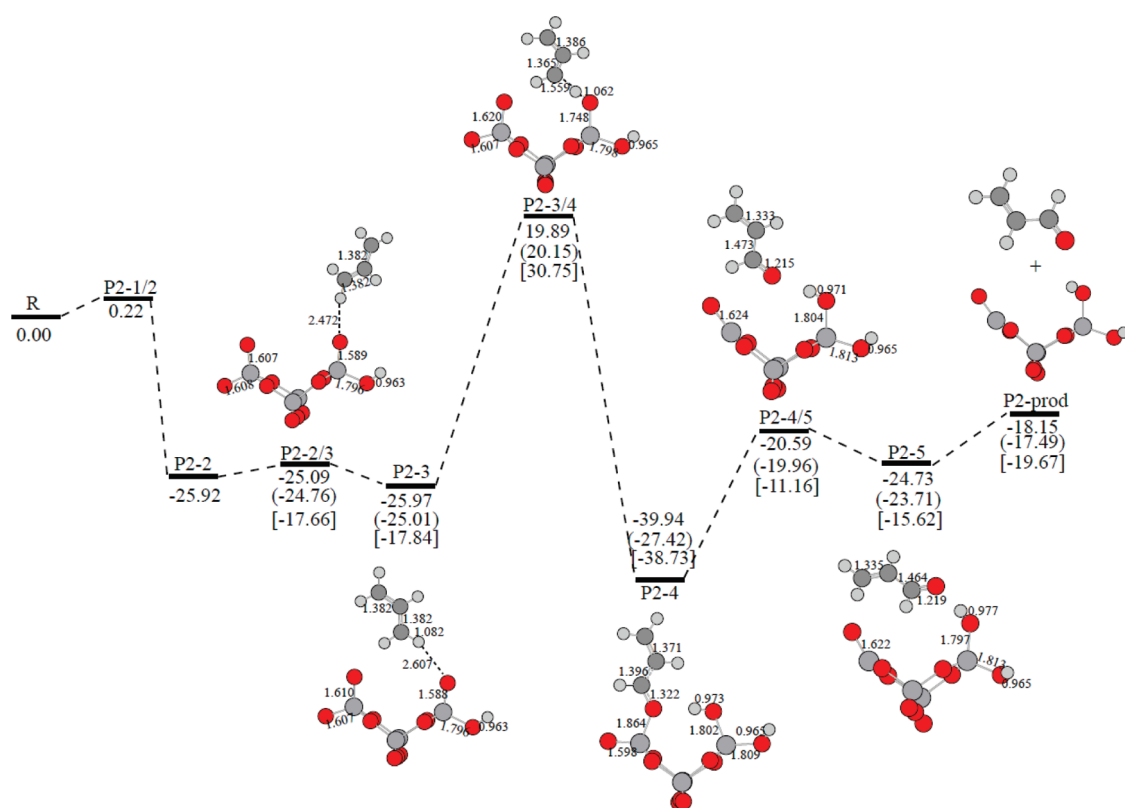


**Figure 3.** The stepwise reactions for path 2. The top energy is the  $\Delta E$  (including ZPE corrections), the middle is  $\Delta H$ , and the bottom is  $\Delta G$ . All reported values are in kcal/mol. Bond distances are shown in angstroms.

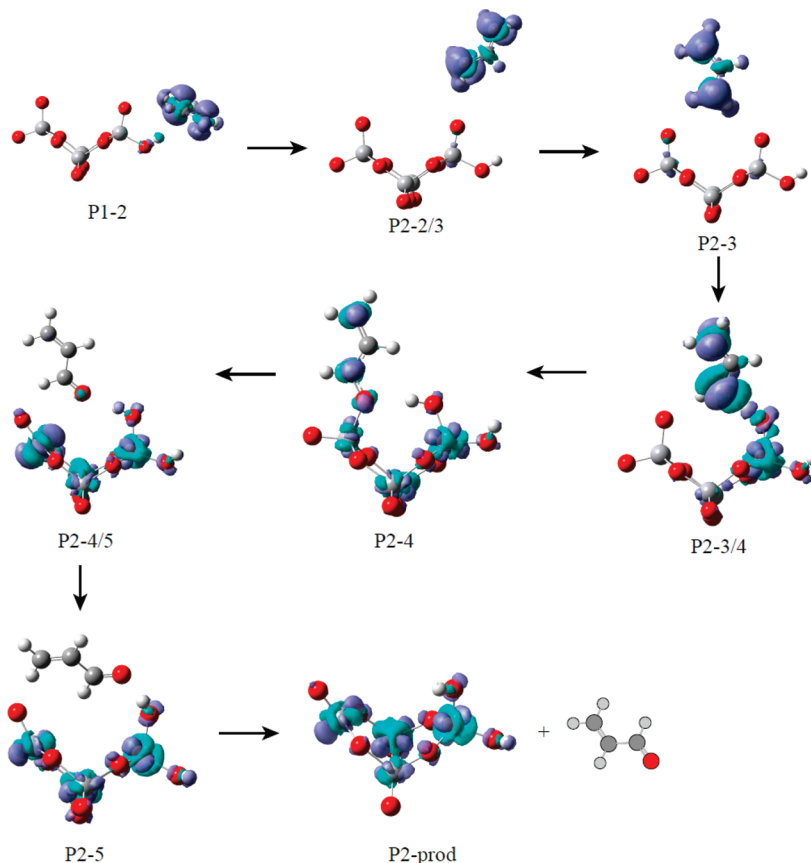


**Figure 4.** Maps of the charge-density difference in the progression of path 2.

mol. Even under a single photon excitation ( $\lambda_{\text{center}} \sim 272$  nm) in the experiment,<sup>8</sup> it is possible that the free energy barrier could be overcome and the first intermediate P1-2, a complex

consisting of [V<sub>4</sub>O<sub>11</sub>•H]<sup>-</sup> cluster and an allyl radical (noted as π-allyl), could be reached. However, the process to P1-2 is exothermic in thermodynamics, that is,  $\Delta H = -25.31$  kcal/

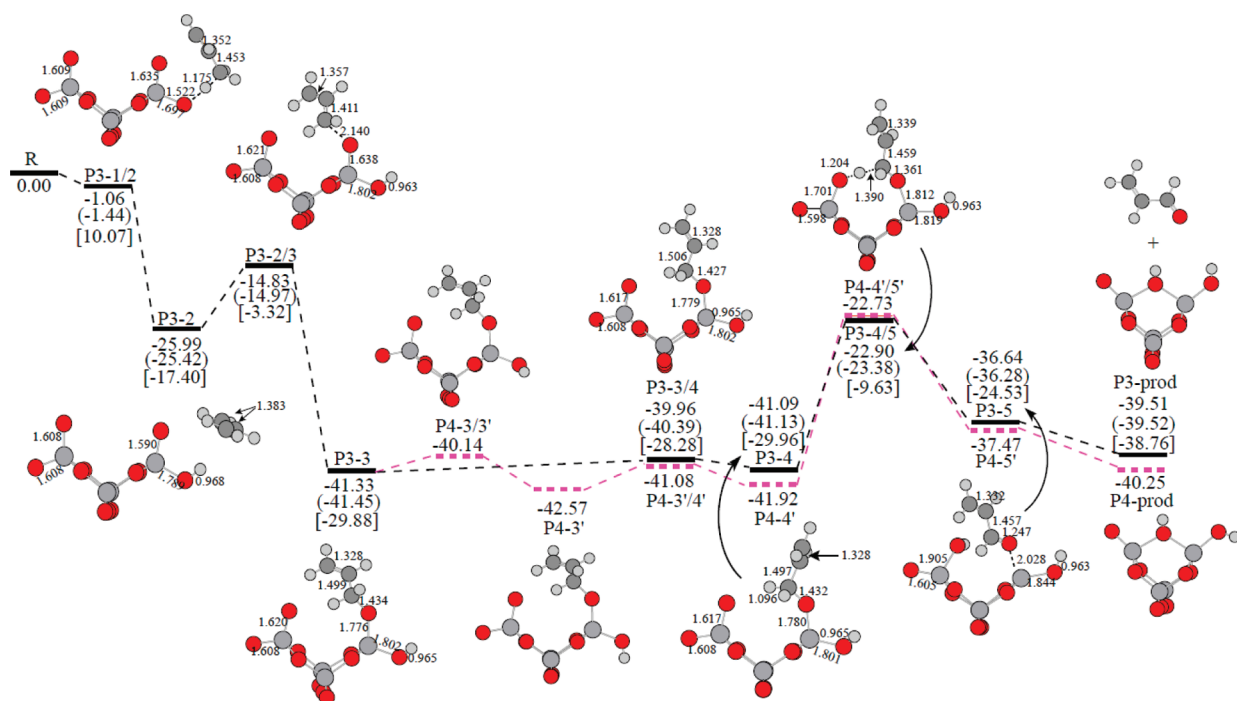


**Figure 5.** The stepwise reactions for paths 3 (solid lines) and 4 (broken lines). The top energy is the  $\Delta E$  (including ZPE corrections), the middle is  $\Delta H$ , and the bottom is  $\Delta G$ . All reported values are in kcal/mol. Bond distances are shown in angstroms.

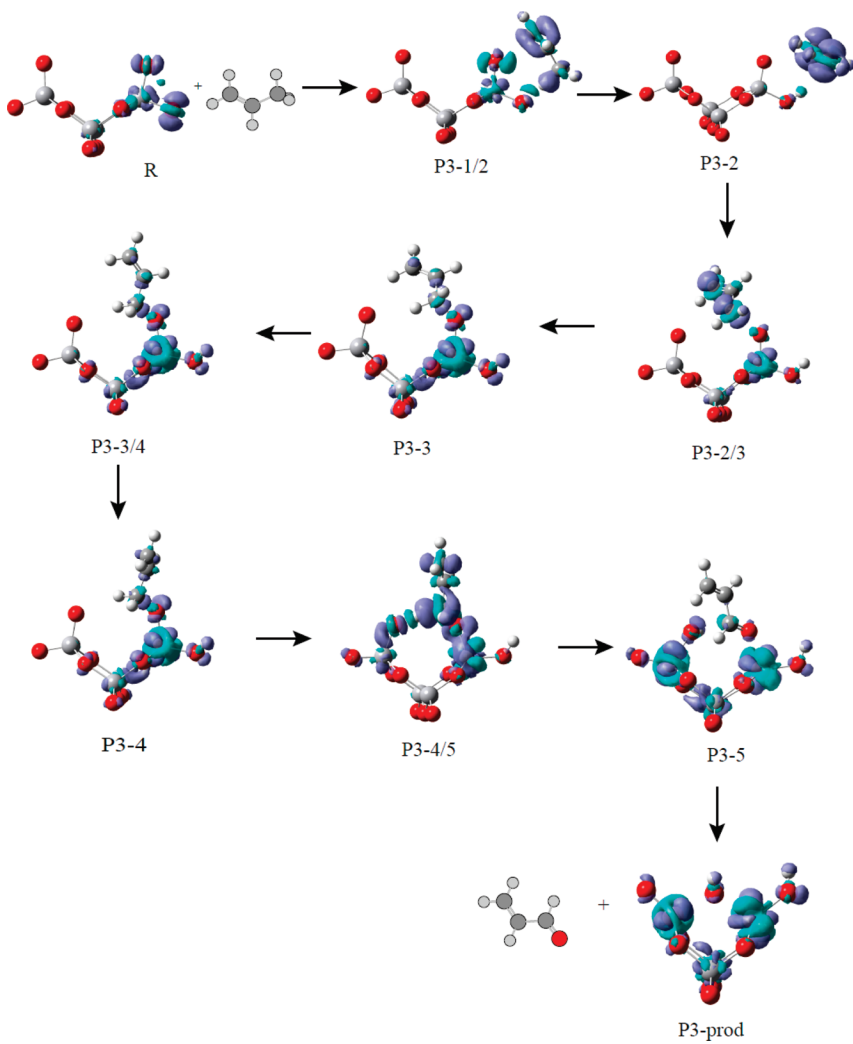


**Figure 6.** Maps of the charge-density difference in the progression of path 3.

mol and  $\Delta G = -17.99$  kcal/mol. Both the TS and intermediate structures for this step in path 2 are exactly as same as those in path 1.

Path 3 also resembles path 1 at the first step, although the relative orientation of propene with respect to the vanadium oxide cluster in path 3 is different from that in path 1. Due to the steric effect of the double-bond C=C, the hydrocarbon is found to rotate around the activated methyl C–H bond in comparison between P1–1/2 and P3–1/2, as well as the different orientations of  $\pi$ -allyl with respect to the vanadium oxide cluster (see Figures 1 and 5). Such steric effect also leads to the distinctly different energy barriers from the reactants to the intermediates. The first TS structure, P3–1/2, in path 3 is 1.06 kcal/mol lower in energy than the total energies of the isolated reactants, whereas P1–1/2 in path 1 is 0.22 kcal/mol higher.<sup>39</sup>

The first three maps in Figures 2 and 6 show the charge-transfers during the hydrogen abstractions in paths 1 (or 2) and 3. Initially, the negative charge localizes at the terminal O1 and O2 atoms, then it transfers to the  $\pi$ -allyl moiety. This negatively charged  $\pi$ -allyl radical is loosely combined with the cluster and then rotates around O2 atom. The  $\pi$ -allyl radical is recombined with the cluster with a weak C–H $\cdots$ O<sub>2</sub>=V<sub>1</sub> hydrogen bond (2.607 Å) in path 2 or with a covalent bond between the terminal carbon and O2 atoms in paths 1 and 3. In the latter two paths, the terminal carbons of  $\pi$ -allyl are more active than the middle carbon, owing to its much more negative charge (more than 40%). A  $\sigma$ -allylic intermediate is formed when one terminal carbon atom is combined with O2 atom (see P1–3 in Figure 1 and P3–3 in Figure 5), together with the negative-charge flowing back to the vanadium oxide cluster (see P1–3 in Figure 2 and P3–3 in Figure 6). However, in contrast to that in path 1 (see Figure 2) and path 3 (see Figure 6), in path 2 one can find that the weak C–H $\cdots$ O<sub>2</sub>=V<sub>1</sub> hydrogen bond does not alter the negative-charge distribution at the  $\pi$ -allyl moiety (see Figure 4). This is a magic point where two different oxidation processes are branching, although the second hydrogen abstraction commonly happens prior to the allyl oxidation in all reaction paths.

**Second Hydrogen Abstraction and Allyl Oxidation.** This step in paths 1 and 3 is similar to each other, namely, the allyl moiety is covalently combined with the cluster during the second hydrogen abstraction (see Figures 1 and 5). In these two paths, one hydrogen atom in the terminal methylene of  $\pi$ -allyl is released and then rebonded with O3 atom in the cluster. In path 2, the second hydrogen abstraction occurs along the C–H $\cdots$ O<sub>2</sub>=V<sub>1</sub> hydrogen bond and a hydroxyl O<sub>2</sub>–H group is formed. This process needs to overcome a high energy barrier,  $\Delta E^\ddagger = 45.86$  kcal/mol, from P2–3 to P2–4. The corresponding energy barriers are much lower: 19.24 kcal/mol for P1–3 to P1–4, 18.19 kcal/mol for P3–4 to P3–5, and 19.19 kcal/mol for P4–4' to P4–5', respectively. Obviously, the covalent bond with the terminal oxygen atom can dramatically reduce the energy barrier for the second hydrogen abstraction, which is partially in agreement with the experimental conclusion that the acrolein formation proceeded via the interaction of a propene molecule with two oxygen atoms on the surface.<sup>21</sup>

As shown in Figure 5, path 4, with respect to path 3, has an additional step of the rotation of the bond O<sub>1</sub>–H. The different orientations of O<sub>1</sub>–H group scarcely influence the energy barrier for the second hydrogen abstraction, but lead to two cage-like tautomers, that is, **3** and **4**, in paths 3 and 4, respectively. The energy difference between these two tautomers is only 0.74 kcal/mol (see Scheme 1), implying that they can be easily interconverted by the O<sub>1</sub>–H bond rotation with energy barrier less than

1 kcal/mol.<sup>40</sup> In path 1, the oxygen (O<sub>2</sub>) transfer results in an open structure **1**; while another open structure, **2**, is produced in path 2. They are higher in energy than the cage-like structures (see in Scheme 1). For two open structures **1** and **2**, one also can see that their isomerization is difficult in dynamics. However, the interconversions from the open structures **1** or **2** to the cage-like structures **3** or **4** are much easier.<sup>40</sup>

The oxidation processes (i.e., oxygen transfers) in paths 1 and 2 are endothermic, whereas those in paths 3 and 4 are exothermic. The second hydrogen abstraction is the rate-determining step in paths 2, 3, and 4, according to the highest energy barriers in their respective paths. However, it is a paradox for path 1 because the active energy 19.24 kcal/mol (P1–3 to P1–4) is comparable (in the computational accuracy) with 22.25 kcal/mol for the oxygen transfer (P1–5 to P1–prod).

In Figures 2, 4, and 6, one can find that the negative charge mostly occupies 3d orbitals of the vanadium atom after the second hydrogen abstraction and oxygen transfer. Therefore, the negatively charged species [V<sub>4</sub>O<sub>10</sub><sup>•</sup>·H<sub>2</sub>]<sup>-</sup> were detected in the mass spectrometry experiment.<sup>8</sup>

**Catalysis Mechanism.** As mentioned above, paths 1, 3, and 4 for the selective oxidation of propene to acrolein have the similar stepwise mechanism (see Scheme 2a). Four key steps are summarized here,

(1) The first step in the oxidation of propene is the abstraction of a hydrogen atom from the methyl group of propene, and the hydrocarbon intermediate  $\pi$ -allyl is formed. Along the C–H $\cdots$ O hydrogen bond, the negative charge is transferred from the vanadyl group to  $\pi$ -allyl.

(2) The  $\pi$ -allyl moiety moves to another terminal O atom and is converted to the intermediate  $\sigma$ -allyl by the formation of C–O covalent bond. The negative charge partly transfers back to the vanadium atom. The present study together with our previous work<sup>9</sup> indicates that charge transfer is significantly important in the catalytic oxidation of the hydrocarbon on the anionic vanadium oxide cluster.

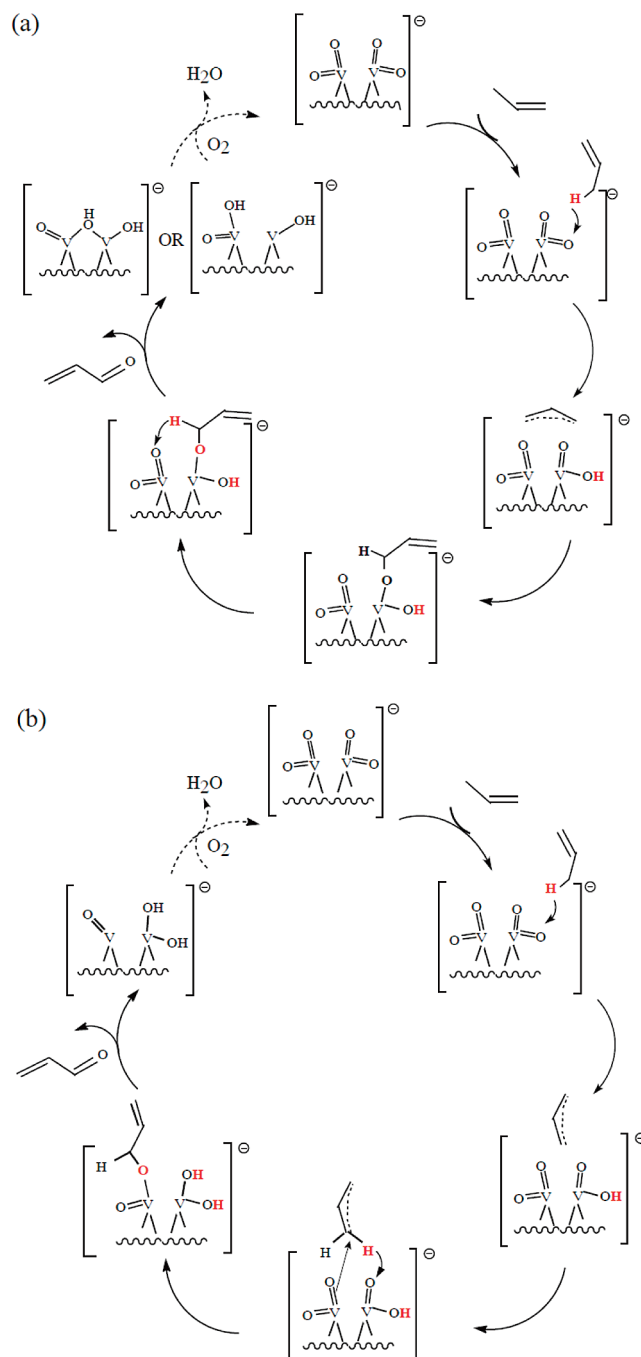
(3) The second hydrogen atom is abstracted by the other V<sub>2</sub>–O<sub>3</sub> group, then the double C=O covalent bond is formed. This step is the rate-determining for these three consecutive reaction pathways.

(4) Acrolein is desorbed from the anionic cluster [V<sub>4</sub>O<sub>10</sub><sup>•</sup>·H<sub>2</sub>]<sup>-</sup>. The negative charge is completely localized at the [V<sub>4</sub>O<sub>10</sub><sup>•</sup>·H<sub>2</sub>]<sup>-</sup> cluster. After the production of acrolein, the anionic [V<sub>4</sub>O<sub>10</sub><sup>•</sup>·H<sub>2</sub>]<sup>-</sup> cluster can be reoxidized by the gaseous oxygen and regenerate the V<sub>4</sub>O<sub>11</sub><sup>-</sup> cluster. This process is favorable in thermodynamics.<sup>41</sup>

On the other hand, path 2 is kinetically unfavorable and has a different mechanism (see Scheme 2b). The distinct difference is that the  $\pi$ -allyl is loosely absorbed on the vanadium oxide cluster, instead of the formation of the  $\sigma$ -allyl intermediate before the second hydrogen abstraction. This results in the high energy barrier for the second hydrogen abstraction.

In the photoinduced experiment,<sup>8</sup> the electron excitations may be involved in the reactions. The femto-second laser pulse was used not only for the product analysis using time-of-flight mass spectrometry but also to stimulate the initial reactions.<sup>8</sup> The stimulations due to electron excitations with the laser pulse (10–160  $\mu$ J,  $\lambda_{\text{center}} \sim 272$  nm)<sup>8</sup> should be considered. We tried to study the excited-state potential surfaces of the reactions with the time-dependent B3LYP/TZVP calculations. However, there are too many excited states within a single photon excitation energy range ( $\lambda_{\text{center}} \sim 272$  nm). Some excited states with large oscillator strengths are lying at the high energies, such as at ca. 3.0 eV (the fifth transition of P1–2) and 2.8 eV (the fourth

**SCHEME 2: Mechanisms of Selective Oxidation of Propene to Acrolein on Anionic  $V_4O_{11}^-$  Clusters: (a) for Paths 1, 3, and 4; (b) for Path 2**



transition of P3–2). More electron transition states are presented as the Supporting Information. It is interesting that the charge transfers in the above electron transitions, that is, the fifth transition of P1–2 and the fourth transition of P3–2 (see the Supporting Information), are similar with the charge transfers for P1–2 → P1–3 (Figure 2) and P3–2 → P3–3 (Figure 6), in good agreement with the original purpose that the charge could be redistributed in the photoinduced experiments.<sup>8</sup> Moreover, there may be the multiphoton excitation effects on the reactions.<sup>8</sup> On the other hand, the products, **1–4**, may be at the different spin states. As shown in Figure S1 (see the Supporting Information), **1** and **2** at doublet states are higher in energy than those at quartet states, whereas **3** and **4** at doublet states are lower in energy than those at quartet states. If the

possibilities of isomerizations among **1–4** are also considered, there may be the various crossing points between the different spin-state potential energy surfaces in the reactions. It is beyond this work to extensively explore the reaction energy surfaces of these excited states, in particular, the various potential crossings. As mentioned above, the initial reactant  $[V_4O_{11}]^\ominus$  is preferred to be at the doublet state in energy, and we aimed to reveal the catalytic mechanism on the doublet-spin potential energy surface in this work.

#### 4. Conclusions

The mechanisms and dynamics of selective oxidation of propene to acrolein on the anionic vanadium oxide cluster  $V_4O_{11}^-$  are investigated by density functional theory calculations. Four possible reaction pathways for the selective oxidation of propene to acrolein on the anionic  $V_4O_{11}^-$  cluster are proposed, commonly indicating a stepwise reaction mechanism. For the energetically favorable paths 1, 3, and 4: first,  $\pi$ -allyl species is produced by the activation of methyl C–H bond and the hydrogen abstraction; second,  $\sigma$ -allyl species is formed by the covalent combination with one terminal oxygen atom; at last, the second hydrogen atom is abstracted by another terminal oxygen atom and acrolein is produced. The last step is rate-determining for the overall reaction pathways. These reaction processes are accompanied with the negative charge transfer between the vanadium oxide cluster and hydrocarbon species. Although the Mars–van Krevelen reaction mechanism<sup>18,23–26,30</sup> was proposed on the basis of the experimental and theoretical studies of the propene oxidation to acrolein catalyzed on the metal oxide surfaces, here we gain more insights into this multistep mechanism with the cluster model.

**Acknowledgment.** This work is partially supported by NSFC (Grant 20673105) and MOST (Grants 2006CB92204 and 2007CB815204). We also thank reviewers for their invaluable comments.

**Supporting Information Available:** Electron excitations of the selected reactants predicted at the time-dependent B3LYP/TZVP level, the optimized geometries of the reactants, TS structures, intermediates, and products, the relative energies of  $[V_4O_{10}\cdot H_2]^\ominus$  at doublet and quartet states. This material is available free of charge via the Internet at <http://pubs.acs.org>.

#### References and Notes

- (1) Ruth, K.; Burch, R.; Kieffer, R. *J. Catal.* **1998**, *175*, 27.
- (2) Weckhuysen, B. M.; Keller, D. E. *Catal. Today* **2003**, *78*, 25.
- (3) Chen, M. S.; Goodman, D. W. *Science* **2004**, *306*, 252.
- (4) Nijhuis, T. A.; Visser, T.; Weckhuysen, B. M. *Angew. Chem., Int. Ed.* **2005**, *44*, 1115.
- (5) Lee, S.; Molina, L. M.; López, M. J.; Alonso, J. A.; Hammer, B.; Lee, B.; Seifert, S.; Winans, R. E.; Elam, J. W.; Pellin, M. J.; Vajda, S. *Angew. Chem., Int. Ed.* **2009**, *48*, 1467.
- (6) (a) Justes, D. R.; Mitič, R.; Moore, N. A.; Bonačić-Koutecký, V.; Castleman, A. W. *J. Am. Chem. Soc.* **2003**, *125*, 6289. (b) Fielicke, A.; Mitič, R.; Meijer, G.; Bonačić-Koutecký, V.; von Helden, G. *J. Am. Chem. Soc.* **2003**, *125*, 15716. (c) Sauer, J.; Döbler, J. *Dalton. Trans.* **2004**, *19*, 3116. (d) Feyal, S.; Schröder, D.; Rozanska, X.; Sauer, J.; Schwarz, H. *Angew. Chem., Int. Ed.* **2006**, *45*, 4677. (e) Feyal, S.; Döbler, J.; Schröder, D.; Sauer, J.; Schwarz, H. *Angew. Chem., Int. Ed.* **2006**, *45*, 4681. (f) Feyal, S.; Schröder, D.; Schwarz, H. *J. Phys. Chem. A* **2006**, *110*, 2647. (g) Bande, A.; Lüchow, A. *Phys. Chem. Chem. Phys.* **2008**, *10*, 3371. (h) Rozanska, X.; Sauer, J. *J. Phys. Chem. A* **2009**, *113*, 11586.
- (7) (a) Dibenedetto, A.; Aresta, M.; Fragale, C.; Distasio, M.; Pastore, C.; Venezia, A. M.; Liu, C.-J.; Zhang, M. *Catal. Today* **2008**, *137*, 44. (b) Dong, F.; Heinbuch, S.; Xie, Y.; Bernstein, E. R.; Rocca, J. J.; Wang, Z.-C.; Ding, X.-L.; He, S.-G. *J. Am. Chem. Soc.* **2008**, *130*, 1932. (c) Rozanska, X.; Kondratenko, E. V.; Sauer, J. *J. Catal.* **2008**, *256*, 84. (d) Rozanska, X.; Sauer, J. *Int. J. Quantum Chem.* **2008**, *108*, 2223.

- (8) Li, S.; Mirabal, A.; Demuth, J.; Wöste, L.; Siebert, T. *J. Am. Chem. Soc.* **2008**, *130*, 16832.
- (9) Li, H.-B.; Tian, S. X.; Yang, J. *Chem. -Eur. J.* **2009**, *15*, 10747.
- (10) Grasselli, R. K. In *Handbook of Heterogeneous Catalysis*; Ertl, G., Knözinger, H., Weitkamp, J., Eds.; VCH: Verlagsgesellschaft mbH, Weinheim, 1997; Vol. V, pp 2303.
- (11) (a) Grasselli, R. K.; Burrington, J. D. *Adv. Catal.* **1981**, *30*, 133. (b) Grasselli, R. K. *Top. Catal.* **2002**, *21*, 79.
- (12) Fattore, V.; Fuhrman, Z. A.; Manara, G.; Notarj, B. *J. Catal.* **1975**, *37*, 223.
- (13) Dadyburjor, D. B.; Jewur, S. S.; Ruckenstein, E. *Catal. Rev.* **1979**, *19*, 293.
- (14) Carbuicchio, M.; Centi, G.; Forzatti, P.; Trifiro, F.; Villa, P. L. *J. Catal.* **1987**, *107*, 307.
- (15) Lieto, J. M.; Bielsa, R.; Kremenic, G.; Fierro, J.; Stud, L. *Surf. Sci. Catal.* **1990**, *55*, 295.
- (16) He, D.; Ueda, W.; Moro-Oka, Y. *Catal. Lett.* **1992**, *12*, 35.
- (17) Schultz, K. H.; Cox, D. F. *J. Catal.* **1993**, *143*, 464.
- (18) Moro-oka, Y.; Ueda, W. *Adv. Catal.* **1995**, *40*, 233.
- (19) Zhao, C.; Wachs, I. E. *Catal. Today* **2006**, *118*, 332.
- (20) (a) Sampson, R. J.; Shooter, D. *Oxid. Combust. Rev.* **1965**, *1*, 225. (b) Voge, H. H.; Adams, C. R. *Adv. Catal.* **1967**, *17*, 151. (c) Sachtler, W. M. H. *Catal. Rev.* **1970**, *4*, 27. (d) Margolis, L. Ya. *Catal. Rev.* **1973**, *8*, 241. (e) Hucknall, D. J. In *Selective Oxidation of Hydrocarbons*; Academic Press: New York, 1974. (f) Arora, N.; Deo, G.; Wachs, I. E.; Hirt, A. M. *J. Catal.* **1995**, *159*, 1.
- (21) Aso, I.; Furukawa, S.; Yamazoe, N.; Seiyama, T. *J. Catal.* **1980**, *64*, 29.
- (22) Burrington, J. D.; Kartisek, C. T.; Grasselli, R. K. *J. Catal.* **1984**, *87*, 363.
- (23) Bielanski, A.; Haber, J. In *Oxygen in Catalysis*; Dekker, M., Eds.; Wiley: New York, 1991, p. 231.
- (24) Bettahar, M. M.; Constantine, G.; Savary, L.; Lavalle, J. C. *Appl. Catal. A* **1996**, *145*, 1.
- (25) Grasselli, R. K. *Catal. Today* **1999**, *49*, 141.
- (26) Doornkamp, C.; Ponec, V. *J. Mol. Catal. A: Chem.* **2000**, *162*, 19.
- (27) Allen, M.; Betteley, R.; Bowker, M.; Hutchings, G. *J. Catal. Today* **1991**, *9*, 97.
- (28) van Steen, E.; Schnobel, M.; Walsh, R.; Riedel, T. *Appl. Catal. A: Gen.* **1997**, *165*, 349.
- (29) Pudar, S.; Osgaard, J.; van Duin, A. C. T.; Chenoweth, K.; Goddard, W. A., III *J. Phys. Chem. C* **2007**, *111*, 16405.
- (30) Zhang, C.; Catlow, C. R. A. *J. Catal.* **2008**, *259*, 17.
- (31) Wang, Z.-C.; Xue, W.; Ma, Y.-P.; Ding, X.-L.; He, S.-G.; Dong, F.; Heinbuch, S.; Rocca, J. J.; Bernstein, E. R. *J. Phys. Chem. A* **2008**, *112*, 5984.
- (32) Frisch, M. J.; Trucks, G. W.; Schlegel, H. B.; Scuseria, G. E.; Robb, M. A.; Cheeseman, J. R.; Montgomery, Jr. J. A.; Vreven, T.; Kudin, K. N.; Burant, J. C.; Millam, J. M.; Iyengar, S. S.; Tomasi, J.; Barone, V.; Mennucci, B.; Cossi, M.; Scalmani, G.; Rega, N.; Petersson, G. A.; Nakatsuji, H.; Hada, M.; Ehara, M.; Toyota, K.; Fukuda, R.; Hasegawa, J.; Ishida, M.; Nakajima, T.; Honda, Y.; Kitao, O.; Nakai, H.; Klene, M.; Li, X.; Knox, J. E.; Hratchian, H. P.; Cross, J. B.; Adamo, C.; Jaramillo, J.; Gomperts, R.; Stratmann, R. E.; Yazayev, O.; Austin, A. J.; Cammi, R.; Pomelli, C.; Ochterski, J. W.; Ayala, P. Y.; Morokuma, K.; Voth, G. A.; Salvador, P.; Dannenberg, J. J.; Zakrzewski, V. G.; Dapprich, S.; Daniels, A. D.; Strain, M. C.; Farkas, O.; Malick, D. K.; Rabuck, A. D.; Raghavachari, K.; Foresman, J. B.; Ortiz, J. V.; Cui, Q.; Baboul, A. G.; Clifford, S.; Cioslowski, J.; Stefanov, B. B.; Liu, G.; Liashenko, A.; Piskorz, P.; Komaromi, I.; Martin, R. L.; Fox, D. J.; Keith, T.; Al-Laham, M. A.; Peng, C. Y.; Nanayakkara, A.; Challacombe, M.; Gill, P. M. W.; Johnson, B.; Chen, W.; Wong, M. W.; Gonzalez, C.; Pople, J. A. *Gaussian 03*; Gaussian, Inc.: Pittsburgh PA, 2003.
- (33) (a) Lee, C.; Yang, W.; Parr, R. G. *Phys. Rev. B* **1988**, *37*, 785. (b) Becke, A. D. *J. Chem. Phys.* **1993**, *98*, 5648.
- (34) Schäfer, A.; Huber, C.; Ahlrichs, R. *J. Chem. Phys.* **1994**, *100*, 5829.
- (35) Santambrogio, G.; Brümmer, M.; Wöste, L.; Döbler, J.; Sierka, M.; Sauer, J.; Meijer, G.; Asmis, K. R. *Phys. Chem. Chem. Phys.* **2008**, *10*, 3992.
- (36) In ref 35, the dioxo-bridge and dioxo-open isomers are the most stable isomers with energy difference only 0.02 eV. In this work, when we adopted these two isomers as the different reactants with propene, their initial complexes and intermediates are identical. Therefore, the dioxo-open conformer V<sub>4</sub>O<sub>11</sub><sup>-</sup> (shown in Scheme 1) is used in this work.
- (37) (a) Fukui, K. *J. Phys. Chem.* **1970**, *74*, 4161. (b) González, C.; Schlegel, H. B. *J. Chem. Phys.* **1989**, *90*, 2154. (c) González, C.; Schlegel, H. B. *J. Phys. Chem.* **1990**, *94*, 5523.
- (38) Driscoll, D. J.; Martin, W.; Wang, J.-X.; Lunsford, J. H. *J. Am. Chem. Soc.* **1985**, *107*, 58.
- (39) When the precursor complex in the reverse direction (to the reactants) was searched using IRC method, a temporary complex [V<sub>4</sub>O<sub>11</sub>•C<sub>3</sub>H<sub>6</sub>]<sup>-</sup> was found, but it was deformed dramatically during the further geometrical optimization. The similar case was also found for P1→1/2. The difficulties in the searching for a stable configuration of [V<sub>4</sub>O<sub>11</sub>•C<sub>3</sub>H<sub>6</sub>]<sup>-</sup> imply that this complex might be on an extremely flat potential energy surface. A weak-bound complex [V<sub>4</sub>O<sub>11</sub>•C<sub>3</sub>H<sub>6</sub>]<sup>-</sup> was postulated to be lower in energy than the TS structure if it has the value close to the total energies of the isolated reactants.
- (40) The energy barriers for the inter-conversions among four isomers [V<sub>4</sub>O<sub>10</sub>•H<sub>2</sub>]<sup>-</sup>: For **1**→**4**, the energy barrier ( $\Delta E$ ) is 6.38 kcal/mol; For **2**→**4**,  $\Delta E$  is 1.48 kcal/mol; For **3**→**4**,  $\Delta E$  is 0.17 kcal/mol; For **1**→**2**, there may be two steps, namely, **1**→**4**→**2**, in which  $\Delta E$  for **4**→**2** is 23.58 kcal/mol.
- (41) For the reactions [V<sub>4</sub>O<sub>10</sub>•H<sub>2</sub>]<sup>-</sup> (x) + O<sub>2</sub> → V<sub>4</sub>O<sub>11</sub><sup>-</sup> + H<sub>2</sub>O. These processes are exothermic: x = 1,  $\Delta H = -68.42$  kcal/mol; x = 2,  $\Delta H = -96.65$  kcal/mol; x = 3,  $\Delta H = -91.23$  kcal/mol.

JP1002947